# Organization and identification of solutions in the time-delayed Mackey-Glass model

Pablo Amil, Cecilia Cabeza, Cristina Masoller, and Arturo C. Martí

## Articles you may be interested in

Design of coupling for synchronization in time-delayed systems
Chaos 22, 033111 (2012); 10.1063/1.4731797

Transient behavior in systems with time-delayed feedback
Chaos 21, 023114 (2011); 10.1063/1.3581161

A simple time-delay feedback anticontrol method made rigorous
Chaos 14, 662 (2004); 10.1063/1.1763014

Theoretical and experimental aspects of chaos control by time-delayed feedback
Chaos 13, 259 (2003); 10.1063/1.1496955

Quasicontinuous control using time-delay coordinates
AIP Conf. Proc. 411, 237 (1997); 10.1063/1.54224

# Organization and identification of solutions in the time-delayed Mackey-Glass model

Pablo Amil,[1] Cecilia Cabeza,[1] Cristina Masoller,[2] and Arturo C. Martí[1]

[1]*Facultad de Ciencias, Universidad de la República, Igua 4225, Montevideo, Uruguay*
[2]*Departament de Fisica i Enginyeria Nuclear, Universitat Politecnica de Catalunya, Colom 11, E-08222 Terrassa, Barcelona, Spain*

Multistability in the long term dynamics of the Mackey-Glass (MG) delayed model is analyzed by using an electronic circuit capable of controlling the initial conditions. The system's phase-space is explored by varying the parameter values of two families of initial functions. The evolution equation of the electronic circuit is derived and it is shown that, in the continuous limit, it exactly corresponds to the MG model. In practice, when using a finite set of capacitors, an excellent agreement between the experimental observations and the numerical simulations is manifested. As the delay is increased, different periodic or aperiodic solutions appear. We observe abundant periodic solutions that have the same period but a different alternation of peaks of dissimilar amplitudes and propose a novel symbolic method to classify these solutions. © *2015 AIP Publishing LLC*. [http://dx.doi.org/10.1063/1.4918593]

**Multistability, i.e., the coexistence of several attractors for a given set of parameters, is a characteristic feature of nonlinear systems, and in particular, of systems with time-delays. One paradigmatic example of time-delayed system is the well-known Mackey-Glass (MG) equation, which models physiological processes, mainly respiratory and hematopoietic (i.e., formation of blood cellular components) diseases. In time-delayed systems, the evolution of the system at a given time not only depends on the state of the system at the current time but also on the state of the system at *previous* times. The dynamics of processes involving time delays, as those studied by MG, is far more complex than that of non-delayed, i.e., instantaneous, systems. Actually, if the dynamics of a system at time *t* depends on the state of the system at a previous time $t - \tau$, the information needed to predict the evolution is contained in the entire interval $(t - \tau, t)$. Thus, the evolution of a delayed system depends on *infinite* previous values of the variables. In mathematical terms, delayed systems are modeled in terms of delayed differential equations (DDEs). The MG model exhibits, as the delay increases, a rich variety of behaviors including periodic and chaotic solutions. Here, using a novel electronic implementation of a MG model, we investigate the organization of the trajectories by varying the initial conditions, and identify and classify the coexisting periodic solutions, both, in observations and in model simulations.**

## I. INTRODUCTION

Chaotic systems are characterized by unpredictable behavior; however, it is well known that they exhibit a certain degree of regularity and structure. Nonlinear systems often display multistability, that is, the coexistence of different attractors for the same set of parameters. From observed noisy time-series that display similar oscillatory patterns, identifying and distinguishing different coexisting attractors are a challenging task, in particular, when noise induces switching among different attractors. Recently, the phenomenon of extreme multistability has been predicted numerically in systems of coupled oscillators[1] and experimental observations in a system of two coupled Rossler-like oscillators were found to be consistent with the numerical predictions: by constructing an electronic circuit representing the system, Patel *et al.*[2] demonstrated a controlled switching to different attractor states through a change in initial conditions only, keeping fixed the system's parameters. While in most multi-stable systems chaotic attractors are rare,[3] systems with time delays are an exception to this rule. A time-delay renders the phase space of a system infinite-dimensional, as one needs to specify, as initial condition, the value of a function, $F_0$, over the time interval $(-\tau, 0)$, with $\tau$ being the delay time. This initial condition is referred to as the initial function (IF). Time-delayed systems often display coexisting, high-dimensional attractors.[4–9]

Time-delays occur in a wide range of real-world systems, either due to couplings or to feedback loops (for recent reviews, see Refs. 10 and 11), and many practical applications have been demonstrated, for example, it has been shown that delay-dynamical systems, even in their simplest manifestation, can perform efficient information processing,[12] and the high dimensionality of the chaotic dynamics that they generate can be exploited for implementing ultra-fast random number generators.[13,14]

A paradigmatic time-delayed system is the Mackey-Glass (MG) model,[15] which exhibits a rich variety of periodic and complex behaviors. The MG model, a first-order nonlinear delayed differential equation, was proposed in 1977 by Mackey and Glass to model physiological systems, mainly respiratory and hematopoietic diseases (i.e., formation of blood cellular components).[15] The onset of these diseases is associated with alterations (bifurcations) in the

periodicity of physiological variables, for example, irregular breathing patterns or fluctuations in peripheral blood cell counts.[16–18]

In this work, we describe an experiment using an electronic circuit designed to mimic the Mackey-Glass delay differential equation. The discrete equations governing the dynamics of the circuit are presented. We show that, in spite of the fact that in the electronic circuit the infinite phase space of the MG system is discretized via a finite set of $N$ values; if $N$ is large enough the electronic circuit is indeed a highly precise implementation of the MG model. Then, we study the multistability of coexisting solutions by distinguishing and classifying different periodic and aperiodic solutions using a symbolic-dynamic algorithm. The agreement between the experimental observations and numerical simulations is verified using cross-correlation functions.

This paper is organized as follows: in Sec. II, the MG model is introduced and previous results discussed. In Sec. III, the Mackey-Glass electronic analog is described, the system to control the IF is presented and the discrete equations of the circuit derived. The results are presented in Sec. IV, the experimental and numerical temporal series and bifurcation diagrams are compared in order to demonstrate that the electronic circuit perfectly reproduces the MG model. In this section, the coexistence of periodic and aperiodic solutions is analyzed and the correspondence with specific analytical results is discussed. Finally, Sec. V presents a summary of the results and the conclusion.

## II. THE MG MODEL

In their original paper,[15] Mackey and Glass considered a population of mature circulating white blood cells. In this physiological process, there is a delay, $\tau$, between the initiation of cellular production in the bone narrow and their release into the blood. The dynamics of the density of blood cells is increasingly complex as the delay grows. When there is no delay, $\tau = 0$, there is a stable equilibrium point which becomes unstable with increasing delay and different periodic solutions appear. As the delay further increases, a sequence of bifurcations generates oscillations with higher periods and eventually aperiodic behavior.[19]

Over the years, the dynamics of the MG model has been investigated numerically,[20–25] and it has been used to generate high-dimensional chaotic signals.[26] The MG model has also been used as a toy model to study chaotic synchronization in delayed systems.[27–29] Another appealing application of the MG model, and also of other systems exhibiting multistability, is the possibility of storing information in the temporal patterns present in the different co-existing solutions. This capability was demonstrated by Lim *et al.* using a hybrid diode laser system.[30]

Several groups have proposed experimental implementations of the MG model via electronic circuits.[5,19,29,31–33] An electronic implementation based on an *analog delay line* was considered in Refs. 19, 28, and 31 to address the problem of synchronization and control of high dimensional chaos. The analog delay line is the electronic analog of a chain of masses and springs and, broadly speaking, generates

an effective delay only for low enough frequencies. This approach was extended in the design proposed in Ref. 34 to analyze synchronization in systems with multiple feedbacks. Digital electronic implementations of other delayed systems, using programmable hardware, were recently proposed in Ref. 32. In this case, it is necessary to convert the signal from the RC circuit to the digital domain, apply the delay and convert back to the analog domain.

Multistability in DDEs and, in particular, in the MG was studied in various papers.[5,35,36] The dependence of the solutions on the initial function in the MG model and in other first order DDEs was investigated by Losson *et al.*[5] They showed, by means of numerical and experimental methods, that the basins of attraction of piecewise constant feedback DDE can possess a complex structure at all scales measurable numerically. Specifically in relation with the MG model, Losson *et al.* focus on a family of sinusoidal IFs, which parameter values give rise to limit cycles either with strictly positive or negative values of the variable. Mensour *et al.*[35,36] focused on the multistability exhibited by first-order DDEs at large delay-to-response ratios with the design of dynamical memory devices in mind. They also showed that a finite message can be stored in a periodic waveform and that its storage capability is enhanced by the control of unstable periodic orbits in the chaotic regime. The scope of the present work is to take advantage of a recently proposed electronic implementation[33] to investigate the coexistence of different, but very similar, high-dimensional periodic and aperiodic solutions.

The Mackey-Glass delay-differential equation, as expressed in the original work, is[15]

$$\frac{dP}{dt} = \frac{\beta_0 \Theta^n P_\tau}{\Theta^n + P_\tau^n} - \gamma P, \tag{1}$$

where $P$ is the density of mature circulating white blood cells, $\tau$ is the delay time, and $P_\tau = P(t - \tau)$. The parameters $\Theta$ and $\beta_0$ and the exponent $n$ are related to the production of white blood cells while $\gamma$ represents the decay rate.

The number of parameters can be reduced by re-scaling the variables $x = P/\theta$ and $t' = t\gamma$. After the re-scaling, a simplified equation for $x(t')$ for the MG model is obtained

$$\frac{dx}{dt'} = \alpha \frac{x_\Gamma}{1 + x_\Gamma^n} - x, \tag{2}$$

where $\Gamma = \gamma\tau$ is the normalized delay time, $\alpha = \beta_0/\gamma$, and $x_\Gamma = x(t' - \Gamma)$.

## III. THE EXPERIMENT

### A. Electronic circuit

The electronic implementation of the MG model, as given by Eq. (2), consists of a RC circuit, delay and function blocks and a system to control the initial conditions. The purpose of the delay block is to copy its input as an output after some delay time while the function block implements the nonlinear function. A schematic view of the circuit is shown in Fig. 1, a detailed description can be found in Ref. 33.
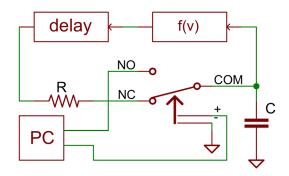
FIG. 1. Experimental setup. The electronic circuit consists of two passive elements, $R$ and $C$, and two blocks, one implements the nonlinear function, $f(v)$, and the other the delay. The initial conditions can be arbitrarily set by using the relay which allows to switch between a free evolution in the NC position, and a controlled evolution in the NO position. The relay state and the voltage in the NC position are controlled by a PC.

The implementation of delay block with analog electronic is possible by employing a *Bucket Brigade Device* (BBD), which is a discrete-time analog device. Internally, it contains an array of $N$ capacitors in which a signal travels one step at a time. The origin of the name comes from the analogy with the term *bucket brigade*, used for a line of people passing buckets of water. In this work, we used the integrated circuits MN3011 and MN3101 as BBD and clock signal generator, respectively.

This approach for implementing a delay approximates the desired transfer function given by $v_{out}(t) = v_{in}(t - \tau)$, by sampling the input signal and outputting those samples $N$ clock periods later. Thus, if $dt$ is the clock period, the delay time is $\tau = N dt$. In the MN3011 $dt$ can vary between $5\,\mu s$ and $50\,\mu s$. The number of capacitors, $N$, can be selected among the values provided by the manufacturer; for our devices, $N = 396, 662, 1194, 1726, 2790$, and $3328$.

The function block, indicated in Fig. 2, was implemented here for an exponent $n = 4$. Other values of $n$ could be similarly implemented. Integrated circuits AD633JN and AD712JN were used to implement sums, multiplications, and divisions because of their simplicity, accuracy, low noise, and low offset voltage. Additional details about the pre- and post-amplification and the evaluation of the inputs and outputs of the delay and the nonlinear functions are described in Ref. 33.

## B. Control of initial conditions

A remarkable advantage of this electronic implementation is that different input signals (i.e., different functions of time) may be selected as initial conditions. As the initial function is fully controlled by the computer, it is easy and straightforward to analyze the evolution of the MG system starting from arbitrary initial conditions.

The initial conditions are given by the voltages in the capacitors, which are defined by an input signal of duration greater than the delay time. A relay synchronized with an analog output of a personal computer (PC) was used as depicted in Fig. 1. This setup allows to switch the system between a free evolution (i.e., the evolution of the electronic model as described: RC circuit, nonlinear function and delay block) in the normal closed (NC) position of the relay, and a controlled evolution in the normal open (NO) position. In this way, with the relay in the NO position, the initial values stored in the delay line (defined by the input signal) were fully controlled by the PC. Then, the relay was set to the NC position, the circuit evolved freely, we measured the voltage immediately after the delay block, and reconstructed the voltage in the capacitor with a tuned digital filter.

## C. Model discretization

By applying Kirchhoff's laws to the circuit shown in Fig. 1 with the relay in the NC position, the equation describing the voltage at the capacitor terminals, $v$, is

$$\frac{dv}{dt} = \frac{1}{RC}\left[ f(v_\tau) - v \right], \tag{3}$$

where $v_\tau = v(t - \tau)$ and $f(v) = \beta \frac{v}{\theta^n + v^n}$, with $\beta$ and $\theta$ circuit constants. Using the definition of the dimensionless time $t' = t\gamma$, setting the characteristic time-scale of the system as $RC = \gamma^{-1}$, and $f$ as the nonlinear function of the MG model, this equation can be identified with Eq. (2).

To analyze whether the electronic circuit described in Sec. III A indeed represents the MG model (i.e., to assess the impact of the implementation of the delay via an array of $N$ capacitors in the Bucket Brigade Device), we first discretize the MG delay-differential equation (as in Eq. (3)) and then compare the simulations of the discretized MG model with observations from the electronic circuit.
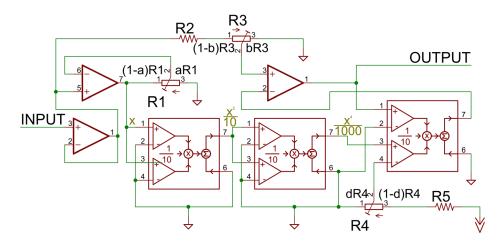


FIG. 2. Electronic implementation of the nonlinear function. Resistor values: $R_1 = 20\,k\Omega$, $R_2 = 56\,k\Omega$, $R_3 = 20\,k\Omega$, $R_4 = 2\,k\Omega$, and $R_5 = 56\,k\Omega$.

The usual way to discretize a delay-differential equation is to approximate the delayed term $f(v_\tau)$ as constant in the small time interval $(t, t+dt)$. In this way, one can integrate Eq. (3) and obtain

$$v(t+dt) = [v(t) - f(v_\tau)]e^{-dt/RC} + f(v_\tau). \quad (4)$$

Denoting $t = jdt$, $\tau = Ndt$, $v_j = v(t)$, and $v_{j-N+1} = v_\tau = v(t-\tau)$, Eq. (4) reads

$$v_{j+1} = [v_j - f(v_{j-N+1})]e^{-dt/RC} + f(v_{j-N+1}). \quad (5)$$

Substituting the expression for the nonlinear function $f(v)$ it results

$$v_{j+1} = v_j e^{-dt/RC} + \left(1 - e^{-dt/RC}\right)\frac{\alpha v_{j-N+1}}{1 + v_{j-N+1}^n}. \quad (6)$$

Equation (6) governs the discrete-time evolution of the electronic circuit. It can be shown that the solutions of this equation tend to the solutions of the original delay-differential equation, Eq. (2), as $dt$ tends to zero and $N$ grows to infinity while the delay time $\tau = Ndt$ is kept constant. Starting with the equation for the dimensionless variable of the MG model

$$\frac{dx}{dt'} = RC\frac{dx}{dt} = RC \lim_{dt\to 0}\left(\frac{x_{j+1} - x_j}{dt}\right), \quad (7)$$

substituting the expression obtained in (6), we obtain

$$\frac{dx}{dt'} = RC \lim_{N\to\infty}\left[\frac{x_j}{dt}\left(e^{-\frac{\Gamma}{N}} - 1\right) + \frac{(1 - e^{-\frac{\Gamma}{N}})}{dt}\frac{\alpha x_{j-N+1}}{1 + x_{j-N+1}^n}\right]. \quad (8)$$

Taking the limit, it results

$$\frac{dx}{dt'} = -RC\Gamma\frac{x(t)}{\tau} + RC\frac{\Gamma}{\tau}\alpha\frac{x(t-\tau)}{1 + x(t-\tau)^n}, \quad (9)$$

reorganizing this expression we obtain

$$\frac{dx}{dt'} = -x(t') + \alpha\frac{x(t'-\Gamma)}{1 + x(t'-\Gamma)^n}, \quad (10)$$

which is exactly the dimensionless continuous-time equation (2).

The agreement between the electronic implementation and the discrete equation, Eq. (5), was checked comparing the temporal series. To consider the worst situation, the smallest possible value of the discretization ($N = 396$) was considered. Clearly, here the most important aspect is to analyze the goodness of the approximation of the delayed term $f(v_\tau)$ as a constant value in the interval $(t, t+dt)$ is, given the specific characteristic time-scales of the electronic circuit.

## IV. RESULTS AND DISCUSSION

### A. Experiment-model comparison

Figure 3 displays two examples of temporal evolutions, one is synthetic, obtained from simulations of Eq. (5), and the
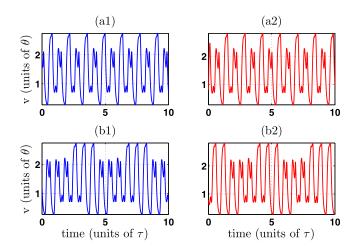


FIG. 3. Comparison between simulations using the discretized solution Eq. (5) (left column) and experimental results obtained from the electronic circuit (right column). The top and bottom rows display coexisting solutions obtained from different initial functions. The parameter values are: $n = 4$, $\alpha = 4.9$, $\Gamma = \tau/RC = 15.7$ and $N = 396$.

other is empirical, recorded from the electronic circuit (the initial conditions are as described in Sec. IV B). One can notice that there is an excellent agreement experiments-simulations: two coexisting solutions were found, both, in the simulations and in the electronic circuit, which are characterized by the same alternation of peaks of different amplitudes.

In Figs. 4 and 5, several examples (empirical and numerical, respectively) time-traces are shown. In these figures, the parameter values of the electronic circuit or the numerical simulations are kept constant while only the initial conditions are varied. To check the quantitative agreement between the experiment and simulations, we calculated the cross-correlation functions. The values of the maxima, the relevant quantity here, are in all the cases in the interval (0.96, 1), revealing the excellent agreement.

Looking at the solutions of Figs. 4 and 5, we distinguish that six are periodic, (a)–(f), and two are aperiodic, (g) and (h). In the periodic time traces, the period (indicated with a black line), is $4.1\tau$ and each period contains precisely 35 maxima. It is remarkable that neither the period, nor the number of maxima per period, uniquely identify the solution. In Sec. IV B, an algorithm designed to characterize these solution is described.

Figures 6 and 7 display bifurcation diagrams and demonstrate that the qualitative agreement is very good for a wide range of normalized delays. These bifurcation diagrams were obtained by plotting, after neglecting transients, the maxima of time series, as a function of $\Gamma = \tau/RC$. In the experimental setup, $\Gamma$ was varied by changing $R$ (i.e., $C$, $N$, and $dt$ were kept fixed).

Looking at the bifurcation diagrams, we observe, in addition to the familiar period-doubling and chaotic branches, singles branches that appear or disappear at certain $\Gamma$ values can be appreciated. These isolated branches are typical of delay-differential equations.[24] We observe here that they appear at the same value of $\Gamma$, both, in the experimental and in the numerical diagram. We can also note that, for the highest $\Gamma$ values, the numerical and experimental
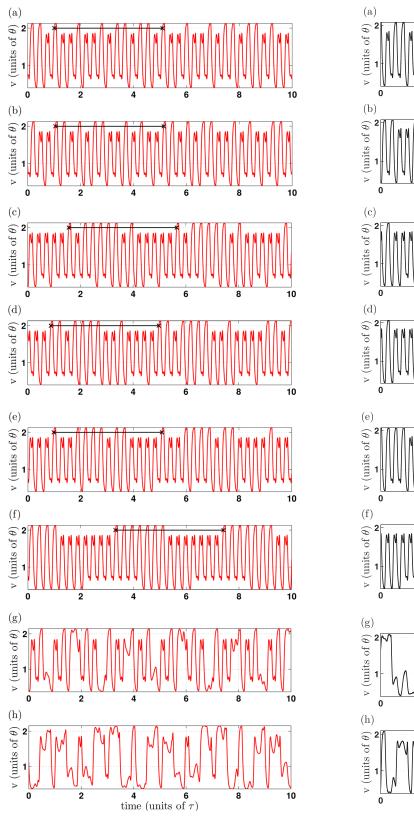
FIG. 4. Periodic and aperiodic experimental time series for the same parameter values and different IFs revealing the multistability of the model. The period, if exists, is indicated with a black line. The parameters of the electronic circuit are $n = 4$, $\alpha = 3.71$, $\Gamma = 40$. The initial function is defined in Eq. (12).
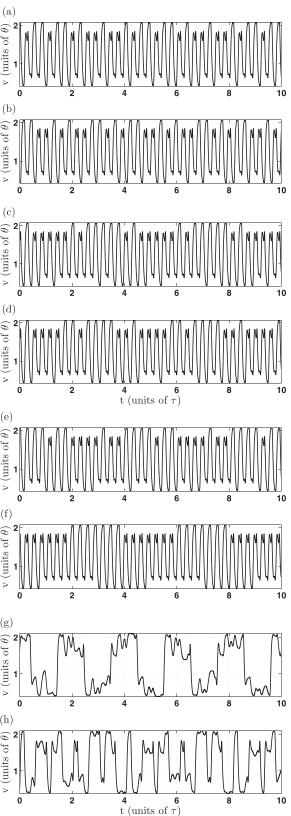


FIG. 5. Continuous time simulations results corresponding to the experimental series shown in Fig. 4. A variable step-size Runge-Kutta (4th–5th) was used integrate the equations. The interpolation of intermediate point was obtained using a cubic spline.

diagrams show a few small differences; this can be expected because the approximation used to derive Eq. (5) [i.e., $f(v_\tau)$ is constant in $(t, t + dt)$], worsens.

To complete the characterization of the model, in Fig. 8 we plot the parameter space as a function of the delay (proportional to $\Gamma$) and the inverse of the decay rate. In color
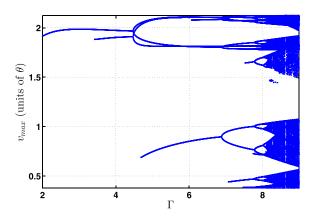
FIG. 6. Bifurcation diagram displaying the maxima of time series, as a function of the normalized delay, $\Gamma = \tau/RC = Ndt/RC$, obtained from simulations of Eq. (6). $\alpha = 3.73$, other parameters are as in Fig. 3.



FIG. 8. Parameter space as a function of the delay and the inverse of the decay rate obtained from numerical simulations of the discrete equation. The number of maxima per period is indicated using the code shown in color bar. Parameter values: $n = 4$, and $N = 396$.

code it is indicated the number of peaks per period of the solution after transient. The initial condition, for this plot, is obtained, at each point, by taking the final values of the previous point. Larger delays result in solutions of increasing number of peaks per period organized in peculiar structures similar to those reported by Junges and Gallas.[24] This figure evidences the richness of the model.

## B. Analysis of multistability

Next, we investigate the influence of the initial conditions. As it is shown in Sec. IV A (see Figs. 3–7), multistability is manifested in a wide range of parameter. In order to identify parameter regions where multi-stability occurs, we developed an algorithm for time-series analysis that allows to unambiguously distinguish similar waveforms.

The analysis algorithm is based in a symbolic representation of a time-series and allows to label the different *periodic* solutions. Two symbols were used, which correspond to highest peaks, and to 2nd highest peaks. analyzed). Once the symbolic string was generated, the algorithm searched for periodicity, and if found, the time-series was labeled with the symbolic string, written in a unique way under cyclic permutations. For example, the symbolic strings *AAABBBAAAABBB* and *BBBAAAABBBBAAA* both represent the
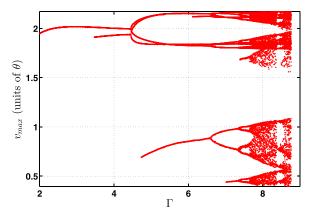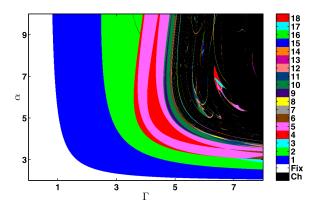
same periodic solution, which has three consecutive high maxima followed by three consecutive smaller maxima. labeling different solutions allows to distinguish among solutions with the same number of peaks per period. The algorithm can be extended to analyze more complex waveforms.

To investigate multi-stability one needs to consider different initial functions, $v(t - \tau) = F_0(t)$ with $t \in (-\tau, 0)$. Here, we consider two families with two parameters each

$$F_0(t) = (v_2 - v_1)\frac{t}{\tau} + v_2, \tag{11}$$

and

$$F_0(t) = \frac{1}{40}\sin\left(\frac{7\pi t}{2\tau} + \phi\right)\sin\left(\frac{7\pi t}{\tau} + 2\phi\right) + v_{\text{off}}, \tag{12}$$

where $(v_1, v_2)$ and $(\phi, v_{\text{off}})$ univocally determine $F_0$ in the interval $(-\tau, 0)$.

Then, for each pair of values, $(v_1, v_2)$ or $(\phi, v_{\text{off}})$, a transient time is neglected (about $5000\tau$ in the simulations and $1000\tau$ in the experiments) and time series of length $200\tau$ (simulations) or $100\tau$ (experiments) are recorded. Their periodicity is analyzed with the symbolic algorithm and the solutions are plotted in the $(v_1, v_2)$ or $(\phi, v_{\text{off}})$ plane. If the MG system is only two-dimensional these plots would identify the basins of attraction of the different solutions; however, the MG system is a delayed system and thus, these plots only classify the different solutions obtained in terms of the two parameters that determine the initial function.

The results are presented in Fig. 9 (where $F_0$ is given by Eq. (11) and the parameters of the MG model and of the electronic circuit are as in Fig. 3) and in Fig. 10 (where $F_0$ is given by Eq. (12) and the parameters are as in Fig. 4). In the first case, there is bistability while in the second case, six different periodic solutions were identified (in Fig. 10, the black regions represent initial functions that result in aperiodic trajectories). Experiments and simulations are contrasted, and again a very good agreement is found. Moreover, we computed the frequency of occurrence of the different coexisting solutions and again a very good agreement was found (not shown). Therefore, our study indicates that, at least for the model parameters considered here, the



FIG. 7. Empirical bifurcation diagram. The electronic circuit delay line has $N = 1194$ $C = 1.0\,\mu$F capacitors. To vary $\Gamma = \tau/RC = Ndt/RC$ within the same range as Fig. 6, $R$ was varied in the range $0.5\,k\Omega$–$1.0\,k\Omega$ and $\alpha = 3.73$, as in Fig. 6.
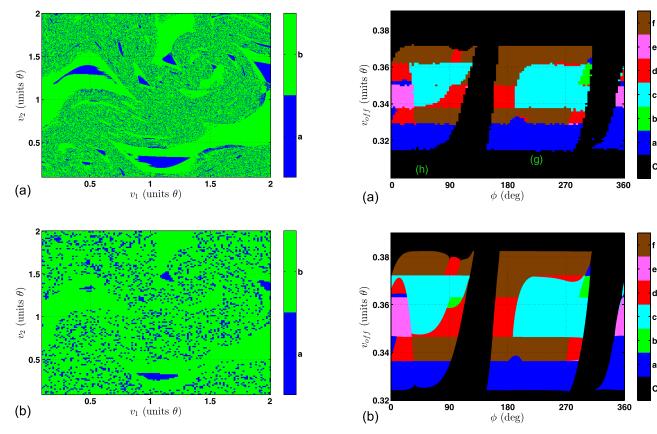
FIG. 9. Map of parameters $(v_1, v_2)$ [that define the initial function given by Eq. (11)], which evolve into one of two possible periodic solutions, *a* in light grey (blue online) or *b* in dark gray (green online). The corresponding waveforms are displayed in Fig. 3. The top panel displays the analysis of simulated time-series while the bottom panel, of empirical data. Parameters are as in Fig. 3.



FIG. 10. As Fig. 9, but now the initial function is defined by Eq. (12), and the parameters are as in Fig. 4. The top panel displays the analysis of simulated time-series while the bottom panel, of empirical data. In both cases, six different periodic waveforms were identified, which are indicated in the color bar with letters *a, b, c, d, e, f* corresponding to the panels in Fig. 4. Aperiodic behavior is indicated in black. The labels *g* and *h* in the map locate the initial conditions that generate trajectories as those displayed in Fig. 4, panels (g) and (f).

electronic circuit reproduces the main features of the MG system (the shape of the waveforms, the bifurcation diagrams, and the maps of bistable and multistable solutions) and thus, it could be used to investigate other issues, for example, noise-induced switching, or how multi-stability affects synchronization.

## C. Discussion

Analytic calculations in time-delayed equations are in general very complex (except in the limit of small delay), and they are beyond the scope of the present work that focuses on an experimental investigation of co-existing time-dependent solutions.

We observe in Figs. 4 and 5 the presence of solutions sharing a common period but the different alternations of *elementary* peaks. These solutions define a family of functions. In the color maps of Figs. 9 and 10 the basin of attraction of two families of these functions are shown. However, it is neither possible to determine a priori the stability of the solutions nor to exclude the existence of other families of periodic or aperiodic solutions.

An interesting observation is that given a solution corresponding to a given delay, this solution is also a solution for other values of the delay. Assuming that, for a set of control parameters, $n$, $\Gamma$, and $\alpha$, there exists a periodic solution of

period $T$: $s(t)$. Then, the solution $s(t)$ is also a solution (not necessarily stable) of an infinite set of control parameters: $n$, $\Gamma_k = \Gamma + kT$, and $\alpha$, where $k$ is an arbitrary integer. Indeed, if $s(t)$ is a solution, it verifies Eq. (2)

$$\frac{ds}{dt}(t) = \alpha \frac{s(t - \Gamma)}{1 + s(t - \Gamma)^n} - s(t) \qquad (13)$$

and thanks to the periodicity

$$\frac{ds}{dt}(t) = \alpha \frac{s(t - kT - \Gamma)}{1 + s(t - kT - \Gamma)^n} - s(t). \qquad (14)$$

By setting $\Gamma_k = \Gamma + kT$, the previous equation becomes

$$\frac{ds}{dt}(t) = \alpha \frac{s(t - \Gamma_k)}{1 + s(t - \Gamma_k)^n} - s(t), \qquad (15)$$

which is the dimensionless equation for the parameters $n$, $\Gamma_k$, and $\alpha$. Then, the solution $s(t)$ is a solution for an infinite set of delay values.

In the discrete-time equation, we can make $\Gamma$ tend to infinity and make some useful insight to the behavior of the system for large delay times. Using the dimensionless version of discrete-time evolution equation, Eq. (5),

$$v_{j+1} = v_j e^{-\frac{\Gamma}{N}} + \left(1 - e^{-\frac{\Gamma}{N}}\right) \alpha \frac{v_{j-N+1}}{1 + v_{j-N+1}^n}, \qquad (16)$$

when making $\Gamma$ tend to infinity the equation becomes

$$v_{j+1} = \alpha \frac{v_{j-N+1}}{1 + v_{j-N+1}^n}, \qquad (17)$$

which could be seen as $N$ independent maps of the form

$$v_{j+1} = \alpha \frac{v_j}{1 + v_j^n}. \qquad (18)$$

These maps exhibit fixed point or oscillatory dynamics depending on the value of the parameter $\alpha$. If $\alpha$ is large enough, the complete solutions consists of $N$ independent maps and, then, corresponds to the case of extreme multistability.

On the other side, if we also consider the continuous limit, $N$ tends to infinity, we recover Eq. (2). Therefore, we conclude that for large delays, the continuous model presents an increasing number of different coexisting solutions.

## V. CONCLUSION

Multistability in the Mackey-Glass (MG) model was studied experimentally, by employing the electronic implementation proposed in Ref. 33, and numerically, by using a discrete-time equation that approximates the exact solutions of the MG model and in particular, models the delay line in the electronic circuit, which is implemented via a linear array of capacitors (a Bucket Brigade Device, BBD). We have found an excellent agreement between observations of the electronic circuit and the simulations of the discrete-time MG model.

In wide parameter regions, different periodic or aperiodic solutions, but with similar waveforms, coexist. In this work, these solutions, exhibiting the alternation of peaks of different amplitudes, were distinguished by means of a symbolic algorithm. A relevant consequence is that, in contrast to other systems in which it is sufficient to count the number of peaks per period (see, for example, Refs. 37 and 38), here, it is necessary to consider the ordering of the peaks to identify the solutions.

The system's phase-space was explored by varying the parameter values of two families of initial functions. The maps of initial conditions that result in different periodic solutions were found to exhibit complex structures, which are not uncommon in delayed systems.[39] A full characterization of the complex organization of these solutions in the system's phase space is an open issue which deserves further research.

The electronic circuit investigated here can be a useful experimental tool for further understanding the bifurcation scenario and the complex solutions of the MG model, and can also be used as "toy model," to study generic features of time-delayed systems, such as deterministic high-dimensional attractors, synchronization in the presence of multistability, or the complex stochastic dynamics that can emerge due to the interplay of multistability, noise, and delay.

[1]C. Hens, R. Banerjee, U. Feudel, and S. Dana, Phys. Rev. E **85**, 035202 (2012).
[2]M. S. Patel, U. Patel, A. Sen, G. C. Sethia, C. Hens, S. K. Dana, U. Feudel, K. Showalter, C. N. Ngonghala, and R. E. Amritkar, Phys. Rev. E **89**, 022918 (2014).
[3]U. Feudel and C. Grebogi, Chaos **7**, 597 (1997).
[4]J. D. Farmer, Physica D **4**, 366 (1982).
[5]J. Losson, M. C. Mackey, and A. Longtin, Chaos **3**, 167 (1993).
[6]J. Foss, A. Longtin, B. Mensour, and J. Milton, Phys. Rev. Lett. **76**, 708 (1996).
[7]C. Masoller, Phys. Rev. A **50**, 2569 (1994).
[8]V. Ahlers, U. Parlitz, and W. Lauterborn, Phys. Rev. E **58**, 7208 (1998).
[9]R. Vicente, J. Daudén, P. Colet, R. Toral *et al.*, IEEE J. Quantum Electron. **41**, 541 (2005).
[10]W. Just, A. Pelster, M. Schanz, and E. Schöll, Philos. Trans. R. Soc., Ser. A **368**, 303 (2010).
[11]V. Flunkert, I. Fischer, and E. Schöll, Philos. Trans. R. Soc., Ser. A **371**, 20120465 (2013).
[12]L. Appeltant, M. C. Soriano, G. Van der Sande, J. Danckaert, S. Massar, J. Dambre, B. Schrauwen, C. R. Mirasso, and I. Fischer, Nat. Commun. **2**, 468 (2011).
[13]A. Uchida, K. Amano, M. Inoue, K. Hirano, S. Naito, H. Someya, I. Oowada, T. Kurashige, M. Shiki, S. Yoshimori *et al.*, Nat. Photonics **2**, 728 (2008).
[14]I. Kanter, Y. Aviad, I. Reidler, E. Cohen, and M. Rosenbluh, Nat. Photonics **4**, 58 (2010).
[15]M. C. Mackey and L. Glass, Science **197**, 287 (1977).
[16]L. Glass and M. C. Mackey, *From Clocks to Chaos: The Rhythms of Life* (Princeton University Press, 1988).
[17]L. Glass, Nature **410**, 277 (2001).
[18]M. C. Mackey and J. G. Milton, Ann. N.Y. Acad. Sci. **504**, 16 (1987).
[19]A. Namajūnas, K. Pyragas, and A. Tamaševičius, Phys. Lett. A **201**, 42 (1995).
[20]X. Ding, D. Fan, and M. Liu, Chaos, Solitons Fractals **34**, 383 (2007).
[21]J. Wei and D. Fan, Int. J. Bifurcation Chaos **17**, 2149 (2007).
[22]A. Wan and J. Wei, Nonlinear Dyn. **57**, 85 (2009).
[23]L. Berezansky, E. Braverman, and L. Idels, Nonlinear Anal.: Theory Methods Appl. **75**, 6034 (2012).
[24]L. Junges and J. A. Gallas, Phys. Lett. A **376**, 2109 (2012).
[25]T. Zhang, Int. J. Biomath. **07**, 1450029 (2014).
[26]P. Grassberger and I. Procaccia, Physica D **9**, 189 (1983).
[27]C. Masoller, Physica A **295**, 301 (2001).
[28]M.-Y. Kim, C. Sramek, A. Uchida, and R. Roy, Phys. Rev. E **74**, 016211 (2006).
[29]S. Sano, A. Uchida, S. Yoshimori, and R. Roy, Phys. Rev. E **75**, 016207 (2007).
[30]T. K. Lim, K. Kwak, and M. Yun, Phys. Lett. A **240**, 287 (1998).
[31]A. Kittel, J. Parisi, and K. Pyragas, Physica D **112**, 459 (1998).
[32]V.-T. Pham, L. Fortuna, and M. Frasca, Nonlinear Dyn. **67**, 345 (2012).
[33]P. Amil, C. Cabeza, and A. C. Martí, IEEE Trans. Circuits Syst. **62** (published online 2015).
[34]T. M. Hoang, T. D. Nguyen, N. V. Duc, J. C. Chedjou, and K. Kyamakya, in *Theoretical Engineering (ISTET), 2009 XV International Symposium on* (VDE, 2009), pp. 1–4.
[35]B. Mensour and A. Longtin, Phys. Lett. A **205**, 18 (1995).
[36]B. Mensour and A. Longtin, Phys. Rev. E **58**, 410 (1998).
[37]C. Cabeza, C. A. Briozzo, R. Garcia, J. G. Freire, A. C. Marti, and J. A. Gallas, Chaos Solitons Fractals **52**, 59 (2013).
[38]J. G. Freire, C. Cabeza, A. Marti, T. Pöschel, and J. A. Gallas, Sci. Rep. **3**, Art. No. 1958 (2013).
[39]M. D. Shrimali, A. Prasad, R. Ramaswamy, and U. Feudel, Int. J. Bifurcation Chaos **18**, 1675 (2008).